# DESIGN AND PERFORMANCE TEST OF DIRECT SEED METERING DEVICE FOR RICE HILL
# /
# *水稻穴直播排种器设计与性能试验*

**Tian Liquan[1, 2], Xiong Yongsen*[1, 2], Ding Zhao[1)], Su Zhan[1)] [1]**

[1)] College of Engineering, Jinhua Polytechnic, Jinhua, 321017 / China

[2)] Key Laboratory of Crop Harvesting Equipment Technology of Zhejiang Province, Jinhua, 321017/China

*Tel: 15888993199; E-mail: tlqbuct@foxmail.com*

*DOI: https://doi.org/10.35633/inmateh-64-25*

***Keywords**: direct seeding in rice hill; seed-metering device; spiral groove; design; test*

## ABSTRACT

*In order to meet the requirements of rice field precision direct seeding in rows and hills, a spiral grooved seed metering device for rice field precision direct seeding in hills is designed. The Matlab software is used to study the movement trajectory of rice buds in the spiral groove during the seeding process. Based on the quadratic regression-orthogonal rotation combination design, and taking the working speed of the seeding wheel, the spiral groove length and the helix angle of the spiral groove as the test factors, as well as the qualified rate of hill diameters, the qualified rate of hill grains and the miss-seeding rate as the indicators, the seed metering performance is tested by JPS-12 metering device test bench. The test data are analyzed by using Design-Expert 6.0.10 software to obtain a mathematical model between the factors and indicators. The test results show that when the spiral groove rise angle is 71.0°, the spiral groove length is 10.8mm, and the working speed of the metering wheel is 23.2r/min, the qualified rate of hill diameter, qualified rate of hill grains and miss-seeding rate are 91.06%, 94.64% and 3.64% respectively. The seeding performance meets the agronomic requirements of rice field seeding.*

## 摘要

*为满足水稻田间精量成行成穴机械直播的要求，设计了一种螺旋槽式水稻田间精量穴直播排种器。应用 Matlab 软件对排种过程中螺旋槽内水稻芽种的运动轨迹进行了研究。采用二次回归正交旋转组合设计，以排种轮工作转速、螺旋槽长度、螺旋槽升角为试验因素，穴径合格率、穴粒数合格率和漏播率为指标，利用 JPS-12 型排种器检测试验台对排种性能进行试验，并运用 Design-Expert6.0.10 软件对试验数据进行分析，得到因素与指标之间的数学模型。试验结果表明：当螺旋槽升角为 71.0°、螺旋槽长度为 10.8mm 和排种轮工作转速为 23.2r/min 时，穴径合格率、穴粒数合格率和漏播率分别为 91.06%、94.64% 和 3.64%，排种性能满足水稻田间播种的农艺要求。*

## INTRODUCTION

Mechanized rice planting mainly includes transplanting and direct seeding. Direct seeding of rice does not require seedlings, and it saves the process of seedlings rising, seedlings pulling and seedlings transplanting during transplantation. It is a labor-saving, cost-saving and energy-saving planting method (*Yin, 2020; Yang, 2020; Wang et al., 2020; Hevko et al., 2018*). Mechanized precision hill direct seeding in the rice field makes the population size of rice field small. Rice plants are evenly distributed in the population, with better ventilation and light transmission, no damage to the root system, well-developed individual root system, more effective tillers, high ear-forming rate and increased yield (*Huang et al., 2020; Dudarev et al., 2017; Arzu and Adnan, 2014*).

Therefore, the precision direct seeding technology of rice that can be used for both rows and hills has become the development direction of mechanized rice planting (*Xing et al., 2020; Xing et al., 2018*). At present, researches on some mechanical seeding technologies, such as rice electromagnetic vibration plug seeding technology, pneumatic suction tube seeding technology, auger seeding technology, seeding belt technology and seed rope technology, have been reported (*Zhang et al., 2018; Liu et al., 2019; Zheng et al., 2018*).

[1] *Tian Liquan, Associate Professor; Xiong Yongsen, Prof; Ding Zhao, Ph.D; Su Zhan, Ph.D;*

However, the structure of seeding device in the above technologies is complex, and the operation is inefficient and the cost is high (*Liu et al., 2017; Zhou et al., 2016*; *Vasylkovska et al., 2019)*. Since 1970s, the research on rice direct seeding metering device has been carried out in China. *Luo et al*. (2008) designed a hill wheel rice direct seeding metering device with two seed filling chambers, but it is difficult to adjust the seeding rate (*Ren et al., 2009; He et al., 2019; Luo et al., 2007*). *Lu et al. (2018)* designed a rice seedling seeder and *Yuan (2006)* developed an air suction vertical tray rice precision seeder (*Lu et al., 2018; Trokhaniak et al., 2020*). The two researches mainly solve the needs of rice transplanting and seedling rising, which is difficult to meet the needs of field direct seeding (*Zhang et al., 2020; Cao et al., 2015*).

In order to meet the requirement of precision seeding and facilitate the adjustment of seeding rate, a spiral grooved seed metering device for rice field precision direct seeding in hills was designed. Its working process was analyzed theoretically and the structural parameters of key components were optimized. Taking the rice seeds as the example, the best combination of various parameters of the seed metering device was obtained to provide a reference for the design of the whole machine.

## MATERIALS AND METHODS

### *Threshed maize mixtures and models of cleaning device*

The structure of the seed metering device is shown in Figure 1. It is mainly composed of a spiral grooved metering wheel, a seed metering wheel cover, a seed cleaning roller brush, a seed protection arc plate, a seed pusher blade, a seed metering wheel positioning sleeve, a cover plate and a sprocket. The seed metering device is installed to the bottom of the seed box through the assembly hill. After determining the working length of the spiral grooved seeding wheel in the metering device (that is, the length of the spiral groove section), fasten the metering wheel positioning sleeve on the main shaft to make the spiral grooved metering wheel unable to move along the axis of the spindle. The seed cleaning sprocket and the driving sprocket are connected by a chain, and the rotation direction of the seed cleaning roller brush and the seed metering wheel are opposite. The seed protection device adopts an elastic seed protection arc plate, so that the short arc surface of the seed protection arc plate is in contact with the seed cleaning roller brush, and the long arc surface is in contact with the spiral grooved seeding wheel. Put the seed pushing blade into the circumferential ring groove cut on the spiral grooved seeding wheel, so that the pushing blade and the bottom of the ring groove are closely attached to improve the seeding effect.

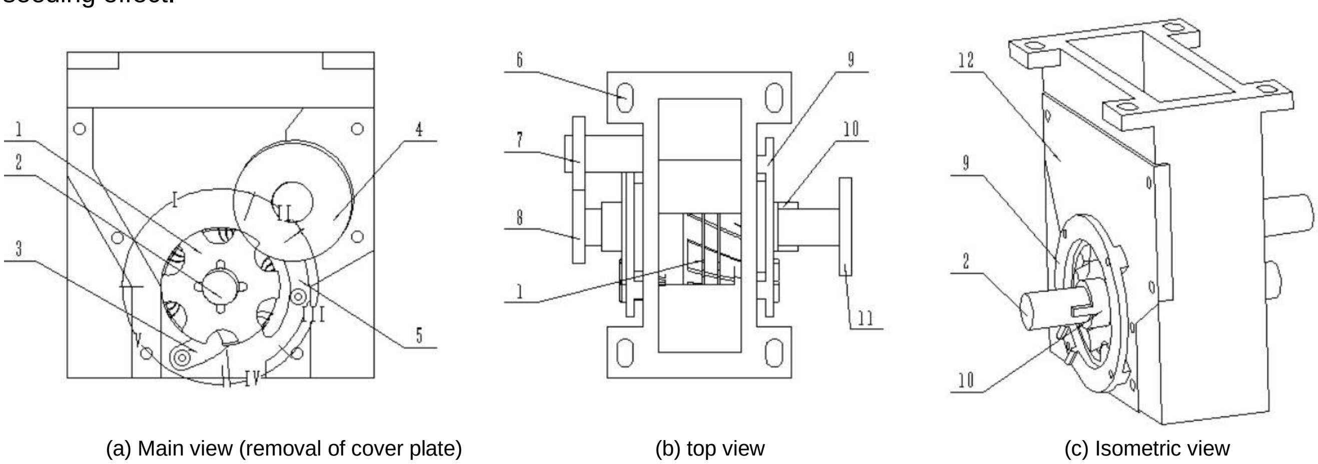


(a) Main view (removal of cover plate) (b) top view (c) Isometric view

**Fig. 1- Sketch of seed-metering device**

I-Filling area II-cleaning area III- Protected area IV-Seeding area V-idle running

*1. Spiral grooved seeding wheel; 2.Spindle; 3.Seed pusher blade; 4.Seed cleaning roller brush; 5.Seed protection arc plate; 6. Upper assembly hole; 7.Seed cleaning sprocket; 8.Drive sprocket; 9. Cover plate of seeding wheel; 10. Positioning sleeve of seeding wheel; 11.Spindle sprocket; 12.Cover plate*

### *Working principle*

Operation of the seed metering device can be divided into four stages: seed filling, seed cleaning, seed protection and seeding. As shown in Figure 1a, the rice buds are filled from the seed box into the seed metering device during operation. The spindle sprocket is powered by the machinery to rotate, and the coaxial drive sprocket drives the clearing sprocket to rotate. In the filling area of the seed metering device, the rice buds are filled into the spiral grooved seeding wheel. The buds filled in the spiral groove enter the seed clearing area with the rotation of the seed metering wheel, and the clearing roller brush removes the excess buds outside the spiral groove hook spoon. The cleared buds remain in the seed filling area for secondary seed filling. After passing through the seed cleaning area, the buds enter the seed protection area with the spiral groove. The seed protection device adopts an elastic seed protection arc plate to ensure the distance between the seed protection arc plate and the seed metering wheel. This cannot only prevent the sprout from getting stuck in the spiral grooved seed metering wheel and the protection arc plate and causes knocks when the distance is too small, but also reduces the abrasion of the buds on the protection arc plate. After passing through the seed protection area, the buds rotate with the seeding wheel to the seeding area; the buds are separated from the spiral groove by the pusher blade and reach the paddy field ground to complete the seeding.

***Design and analysis of key components of the seed metering device***

*Spiral grooved seeding wheel*

The spiral grooved seeding wheel is one of the key components of the seed metering device, and the design of its structural shape and size parameters directly affects the seeding performance. As shown in Figure 2, the seeding wheel is composed of a spiral groove section I and a cylindrical section II with the same diameter. The spoons of the spiral groove section are evenly distributed on the cylindrical surface according to the spiral line pattern. A number of circumferential ring-shaped shallow grooves are cut on the spiral groove section. A spindle hole is set in the center of the seeding wheel, which moves along the spindle through the hole. The positioning sleeve can adjust the length of the spiral groove section in the seeding shell, thereby achieving the purpose of adjusting the seeding volume.

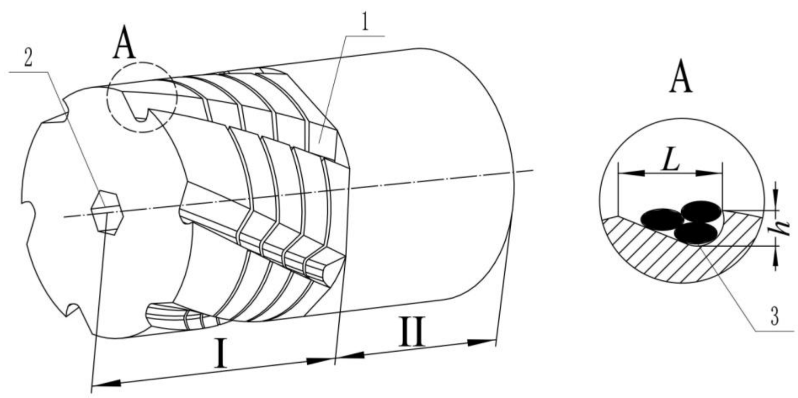


**Fig.2-Sketch of seeding wheel**

*1. spiral groove; 2.spindle hole; 3.buds*

The cross section of the spiral groove segment is a spoon profile formed by arc lines. Where, $L$ is the opening width of the spoon profile, and its value is determined by the length of the longest rice buds. The opening width of the spoon should be 1.1 times the maximum length of buds. $h$ is the depth of spoon, its size affects the uniformity of the seeding wheel, and the value should be greater than the maximum value of the thickness and width of the buds. In order to ensure that at least 3 buds are filled into the spoon, the depth h of the spoon should be 1.4 times the maximum thickness and width of the buds. In order to facilitate the filling and discharge of rice buds from the spoon, the design principle of the contour parameters of the hook-spoon is as follows:

$$\begin{cases} L = 1.1\ l_{max} \\ h = 1.4\ w_{max} \end{cases} \tag{1}$$

where: $l_{mxa}$—Maximum length of rice buds, mm; $w_{max}$—Maximum depth of rice buds, mm.

In order to increase the adaptation range of the spoon-shaped profile of the spiral groove, and optimize the design of reasonable structural parameters, the rice seed Longjing 36 that has a wide range of direct seeding in Heilongjiang was selected. 1000 seeds were randomly selected and soaked to promote germination, so as to make them appear white.

The material characteristics of the buds were measured, and the average value of statistical data and more are shown in Table 1.

The diameter of seeding wheel and the spoons of spiral grooved seeding wheel are important factors that affect the quality of seeding. The single-factor pre-test shows that the diameter of the seeding wheel is small, and the number of evenly distributed spiral grooved scoops is also small. To ensure the required hill spacing during seeding, the rotation speed of the seeding wheel needs to be increased *(Liu et al., 2019)*. However, the rotation speed of the seeding wheel is too large, the time for the spiral grooved spoon to pass through the filling area becomes short, and the buds cannot be filled into the spoon in time, which easily causes miss-seeding. Therefore, the diameter of the seeding wheel should be large. However, too large diameter of seeding wheel will result in the increase of size and mass of the seed metering device. Therefore, the radius of the seed metering wheel is 40mm, and the spiral grooved spoons are 6.

**Table 1**

**Material Characteristics of Longjing36**

| Parameter | Value |
|---|---|
| Quality of thousand grains (kg) | $36.7\times10^{-3}$ |
| Moisture content (%) | 21.8 |
| Natural angle of repose (°) | 36.6 |
| Length×width×thickness / (mm×mm×mm) | 8.08×3.26×2.29 |

***Dynamic analysis of seed filling of spiral grooved spoon***

With the rotation of the seeding wheel, the water rice sprouts and seeds in the seed filling area are driven by the outer wall of the spiral groove and filled into the spoon. There should be a velocity difference between the tangential of the spiral grooved spoon and the outer wall of the spoon, otherwise the normal seed filling of the spoon cannot be guaranteed. Meanwhile, the time for the buds to enter the spiral grooved spoon is one of the main factors affecting the filling performance. If the time that buds enter the spiral grooved spoon is too long, they cannot quickly enter the spiral grooved spoon, resulting in insufficient seed filling and increasing the miss-seeding rate. Therefore, it is necessary to analyze the filling process and explore the relationship between the design parameters of the spiral grooved spoon, the parameters of the buds and the filling time. The coordinate system is established with the centroid of the buds as the coordinate origin and the normal direction of the spiral groove section as the x-axis, as shown in Figure 3.

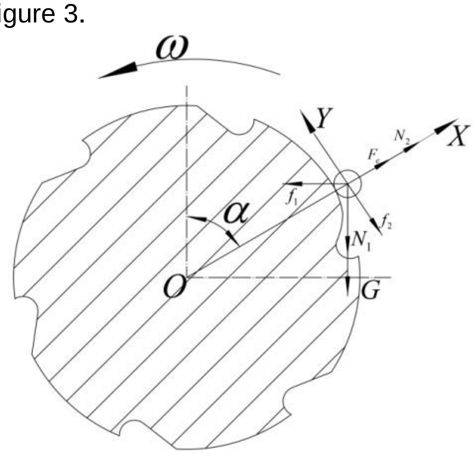


**Fig. 3 - Stress sketch of spoon in the seed-filling process**

To simplify the analysis, this article assumes that the rice buds are spherical and arranged regularly, the pressure on the buds is the sum of the gravity of all the above buds, and the lateral pressure is zero. According to the working conditions of the seed metering device, it can be known that the rice buds are filled into the spoon under the combined action of the gravity $G$, *the* centrifugal force $F_e$, the supporting force between the spiral grooved spoon and the buds $N_1$, the supporting force of the spiral grooved spoon on the buds, the friction force between the outer wall of the spiral grooved spoon and the buds $f_2$, as well as the internal friction $f_1$.

Decompose the force system to the normal and tangential directions of the cross section of the spiral grooved spoon, and establish a mechanical equilibrium equation:

$$\begin{cases} ma_x = (G+N_1)\cos\alpha + f_1\sin\alpha - F_e - N_2 \\ ma_y = (G+N_1)\sin\alpha - f_1\cos\alpha + f_2 \\ f_1 = \mu_1 N_1 \\ f_2 = \mu_2 N_2 \\ F_e = mr\omega^2 \\ G = mg \end{cases} \tag{2}$$

where:

$m$—quality of rice buds, kg; $a_x$—the normal acceleration of rice buds, m/s²;

$a_y$—the tangential acceleration of buds, m/s²;

α—the angular displacement of buds, ( °);

$r$—the distance from the centroid of the buds to the center of the spiral grooved spoon, mm;

$\omega$—the angular velocity of buds, r/min;

$\mu_1$— the friction factor between buds;

$\mu_2$—the friction factor between the outer wall of the spiral grooved spoon and the buds.

It can be obtained by updating Eq.(2) that:

$$\begin{cases} a_x = \dfrac{(mg+N_1)\cos\alpha + \mu_1 N_1\sin\alpha - N_2}{m} - r\omega^2 \\ a_y = \dfrac{(mg+N_1)\sin\alpha - \mu_1 N_1\cos\alpha + \mu_2 N_2}{m} \end{cases} \tag{3}$$

Analyzing the process of rice buds filling the spiral grooved spoon, it can be seen that the relationship between the displacement *h* of the centroid of the buds along the normal direction of the cross section of the spiral grooved spoon and the normal acceleration of the buds is as follows:

$$h = \frac{1}{2}a_x t^2 \tag{4}$$

where:

$h$— the depth of the spiral grooved spoon, mm;

$t$—the time that the centroid of the buds fills into the spiral grooved spoon, s.

Combine Eq.(3) and Eq.(4), it is obtained that:

$$t = \sqrt{\frac{2hm}{(mg+N_1)\cos\alpha + \mu_1 N_1\sin\alpha - mr\omega^2 - N_2}} \tag{5}$$

In order to ensure that the rice buds are fully filled into the spiral grooved spoon, it is necessary to shorten the time for the buds to enter the spiral grooved spoon. According to Eq.(5), it can be seen that after determining the angle α of the filling area, the time *t* for the rice buds to fill the spiral grooved spoon is related to the budding parameters $m$ and $\mu_1$ , as well as the design parameters *h, r* and $\omega$ of the spiral grooved spoon.

### *Helix angle of the spiral groove*

The movement of rice buds in the spiral groove can be divided into the axial movement and the radial rotation along the spiral grooved seed metering wheel. Decompose the speed of the bud M in the spiral grooved spoon at point A, when the lead angle θ of spiral groove is in the unfolded state, the spiral line is represented by an oblique straight line, as shown in Figure 4.

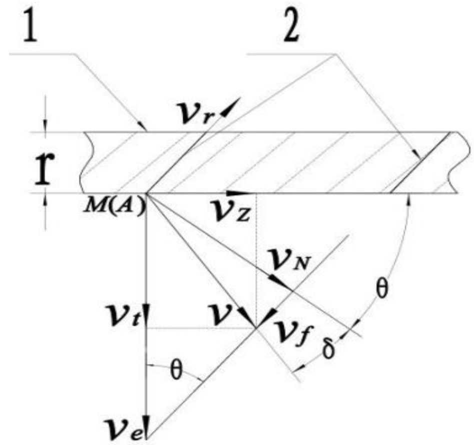


**Fig. 4 - Particle velocity of buds**
*1. Axis; 2. Helix*

The spiral grooved spoon rotates around the axis, and the direction of the linear velocity $v_e$ of the bud $M$ at point $A$ is the tangential direction of this point, which is the implicated speed of the bud. $v_r$ is the relative velocity, and its direction is parallel to the helix direction of point $A$. If the friction of the spiral groove is not taken into account, the bud will move along the normal direction of point $A$ of the spiral line at the theoretical absolute velocity of $v_N$. However, due to the friction of the spiral groove, the actual absolute velocity $v$ of the bud at point $A$ will deflect an angle, which is approximately equal to the external friction equivalent angle $\delta$ of bud grains. The actual absolute velocity $v$ is decomposed into the circumferential velocity $v_t$ and the axial velocity $v_Z$ of the bud, and it is obtained that:

$$\begin{cases} v_z = v\cos(\theta+\delta) \\ v_t = v\sin(\theta+\delta) \end{cases} \tag{6}$$

As shown in Figure 4, without considering the influence of friction, the theoretical absolute speed of buds has:

$$v_N = v_e + v_r \tag{7}$$

Due to the influence of the friction of the spiral groove, the relationship between the actual absolute velocity $v$ and $v_N$ as well as the deflection velocity $v_f$ of the bud at point A is:

$$v = v_f + v_N \tag{8}$$

It can be obtained by velocity triangle that:

$$v = \frac{v_N}{\cos\delta} = \frac{v_e \sin\theta}{\cos\delta} \tag{9}$$

The transport velocity of rice bud at point $A$ is:

$$v_e = \omega r = \frac{2\pi n r}{60} \tag{10}$$

Substituting Eq.(7),-Eq.(10) into Eq.(6), it can be obtained that:

$$\begin{cases} v_z = \dfrac{2\pi r n}{60}\dfrac{\sin\theta}{\cos\delta}\cos(\theta+\delta) \\ v_t = \dfrac{2\pi r n}{60}\dfrac{\sin\theta}{\cos\delta}\sin(\theta+\delta) \end{cases} \tag{11}$$

where:

$n$—rotation velocity of spiral grooved seed metering wheel, r/min.

From Eq. (11), when the rotation speed of the spiral grooved seeding wheel, the distance between the centroid of the rice bud and the center of the spiral groove, as well as the equivalent angle of external friction are determined, the trend of $v_z$ and $v_z$ as the helix angle of spiral groove increases is drawn using Matlab software. The curve is shown in Figure 5.

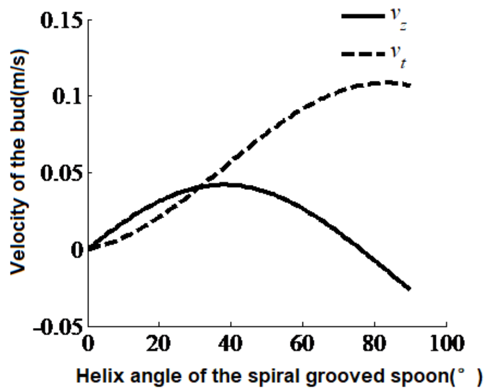


**Fig. 5 - The curve of axial velocity and circumferential velocity**

It can be seen from Figure 5 that with the increase of the helix angle, the axial velocity of rice buds first increases and then decreases. The circumferential velocity increases gradually. In a certain range of helix angle, the axial velocity $V_Z$ and circumferential velocity $V_T$ can be obtained, which makes the axial velocity small and reduces the variation coefficient of the hill diameter. The high circumferential velocity is beneficial to the smooth discharge of buds from the spiral grooved spoon. Therefore, according to the agricultural machinery design manual and the above analysis, when the seed metering performance test is carried out, the range of the spiral groove rise angle θ is 40°-86°.

***Test***

*Test materials*

In order to explore the influence of the velocity of seeding wheel, the spiral groove length and the helix angle of the spiral groove on the seeding performance, and to obtain the best working parameters, a bench test was carried out on the seed metering device, as shown in Figure 6.


**Fig. 6 - The rack experiment of seed-metering device**

*1. seed-metering device; 2. mounting frame; 3. seed bed belt; 4. control motor*

The experiment was conducted in the laboratory of seed metering performance of Northeast Agricultural University, and Longjing 36 was used in the experiment. The rice seeds need to be soaked to promote germination, so as to break the chest and expose white. The test device is the JPS-12 seed metering device detection test bench. The seed metering device is fixed on the mounting frame; the motor is controlled to drive the seed bed belt to rotate, and the seed bed belt is coated with a certain width of sticky seed oil. The rice buds are dropped from the seeding port to the sticky seed oil layer, and data can be collected in real time to achieve the purpose of measuring the performance indicators of various seeding.

*Test factors and indicators*

The working speed of metering wheel and spiral groove angle are the important factors that affect the axial and circumferential speed of bud. At the same time, the change of spiral groove length also has an important impact on the mass of seed metering. Therefore, the working speed of the seeding wheel, the length of the spiral groove and the helix angle of the spiral groove are selected as the test factors, combined with the GB/T6973-2005 " Testing methods of single seed drills (precision drills)", the percentage of the hills with 3-8 buds to the total number of hills is regarded as the qualified rate of hill grains. The percentage of hills with a diameter of less than 50mm and the total number of hills is regarded as the qualified rate of the hill diameter. The qualified rate of the hill grains, the qualified rate of hill diameter and the miss-seeding rate are regarded as the valuation indexes of seeding *(Liu et al., 2019)*.

## RESULTS

### *Experiment design and result analysis*

Firstly, a single-factor pre-test was carried out on the working speed of the seeding wheel, the length of the spiral groove and the lead angle of the spiral groove to determine the reasonable variation range of each factor. On this basis, the three-factor quadratic regression orthogonal rotation combination design is used for experimental analysis. The level codes of the experimental factors are shown in Table 2.

**Table 2**

**Coding level of experimental factors**

| Code | Working speed $x_1$/(r/min) | Spiral length $x_2$/ (mm) | Spiral helix angle $x_3$/ (°) |
|---|---|---|---|
| 1.682 | 30 | 12 | 86 |
| 1 | 27.6 | 10.8 | 76.7 |
| 0 | 24 | 9 | 63 |
| -1 | 20.4 | 7.2 | 49.3 |
| -1.682 | 18 | 6 | 40 |

23 sets of experiments were designed according to the quadratic regression-orthogonal rotation combination, and the experimental schemes and results are shown in Table 3. Among them, $y_1$ is the qualified rate of hill diameter, $y_2$ is the qualified rate of hill grains, and $y_3$ is the miss-seeding rate of hill grains.

**Table 3**

**Schemes and results of experiment**

| No. | Test factors | | | Performance index | | |
|---|---|---|---|---|---|---|
| | $x_1$ (r/min) | $x_2$ (mm) | $x_3$ (°) | $y_1$ (%) | $y_2$ (%) | $y_3$ (%) |
| 1 | 20.40 | 7.20 | 49.30 | 89.16 | 87.13 | 6.28 |
| 2 | 27.60 | 7.20 | 49.30 | 88.95 | 85.09 | 7.86 |
| 3 | 20.40 | 10.80 | 49.30 | 90.87 | 87.24 | 8.2 |
| 4 | 27.60 | 10.80 | 49.30 | 90.25 | 84.56 | 9.2 |
| 5 | 20.40 | 7.20 | 76.70 | 89.74 | 87.45 | 8.22 |
| 6 | 27.60 | 7.20 | 76.70 | 87.97 | 87.55 | 7.38 |
| 7 | 20.40 | 10.80 | 76.70 | 91.31 | 91.97 | 4.36 |
| 8 | 27.60 | 10.80 | 76.70 | 89.76 | 89.71 | 7.18 |
| 9 | 18.00 | 9.00 | 63.00 | 90.33 | 76.74 | 7.48 |
| 10 | 30.00 | 9.00 | 63.00 | 88.54 | 72.41 | 5.18 |

**Table 3**
**(Continuation)**

**Schemes and results of experiment**

| No. | Test factors | | | performance index | | |
|---|---|---|---|---|---|---|
| | $x_1$ (r/min) | $x_2$ (mm) | $x_3$ (°) | $y_1$ (%) | $y_2$ (%) | $y_3$ (%) |
| 11 | 24.00 | 6.00 | 63.00 | 88.08 | 94.1 | 2.32 |
| 12 | 24.00 | 12.00 | 63.00 | 91.04 | 94.07 | 4.8 |
| 13 | 24.00 | 9.00 | 40.00 | 89.41 | 88.1 | 9.06 |
| 14 | 24.00 | 9.00 | 86.00 | 90.28 | 93.32 | 6.3 |
| 15 | 24.00 | 9.00 | 63.00 | 91.05 | 93.41 | 3.2 |
| 16 | 24.00 | 9.00 | 63.00 | 90.40 | 90.13 | 2.74 |
| 17 | 24.00 | 9.00 | 63.00 | 90.71 | 88.31 | 3.32 |
| 18 | 24.00 | 9.00 | 63.00 | 90.54 | 91.2 | 3.72 |
| 19 | 24.00 | 9.00 | 63.00 | 90.76 | 90.38 | 3.96 |
| 20 | 24.00 | 9.00 | 63.00 | 91.11 | 90.82 | 3.04 |
| 21 | 24.00 | 9.00 | 63.00 | 90.59 | 94.04 | 5.46 |
| 22 | 24.00 | 9.00 | 63.00 | 90.64 | 89.72 | 3.2 |
| 23 | 24.00 | 9.00 | 63.00 | 90.70 | 93.63 | 5.5 |

Regression analysis was performed on the test data through Design-Expert 6.0.10 software, the significant influencing factors were screened out, and the corresponding regression equation was obtained.

$$y_1 = 46.97 + 1.78x_1 + 2.51x_2 + 0.34x_3 - 6.31x_1x_3 - 0.03x_1^2 - 0.11x_2^2 - 0.001x_3^2 \tag{12}$$

$$y_2 = -108.42 + 20.51x_1 - 9.14x_2 - 0.21x_3 + 0.04x_2x_3 - 0.43x_1^2 + 0.40x_2^2 \tag{13}$$

$$y_3 = 71.55 - 4.34x_1 + 2.47x_2 - 0.82x_3 - 0.04x_2x_3 + 0.09x_1^2 + 0.01x_3^2 \tag{14}$$

The response surface graph is shown in Figure 7 by Design-Expert 6.0.10 software.

Analysis of the above regression equation and response surface graph shows that the interaction between the spiral groove length and the helix angle of spiral groove has a significant impact on the number of hills and the miss-seeding rate. The interaction between the helix angle of spiral groove and the working speed of the metering wheel has a significant impact on the qualified rate of hill diameter.

It can be seen from Figure 7a that when the helix angle is constant, the qualification rate of hill diameters first increases and then decreases with the increase of working speed; when the working speed is constant, the qualified rate of hill diameters increases with the increase of helix angle. This result is consistent with the previous analysis of the influence of the helix angle of spiral groove on the axial velocity of rice buds.

It can be seen from Figure 7b that when the length of the spiral groove is constant, the qualified rate of hill grains first decreases and then increases with the increase of the spiral helix angle; when the spiral rise angle is constant, the qualified rate of hill grains decreases with the increase of the spiral groove length.

It can be seen from Fig. 7c that when the length of the spiral groove is constant, the miss-seeding rate first decreases and then increases with the increase of the helix angle; when the length changes, the miss-seeding rate varies widely, so the length of the spiral groove is the main factor affecting the leakage rate.

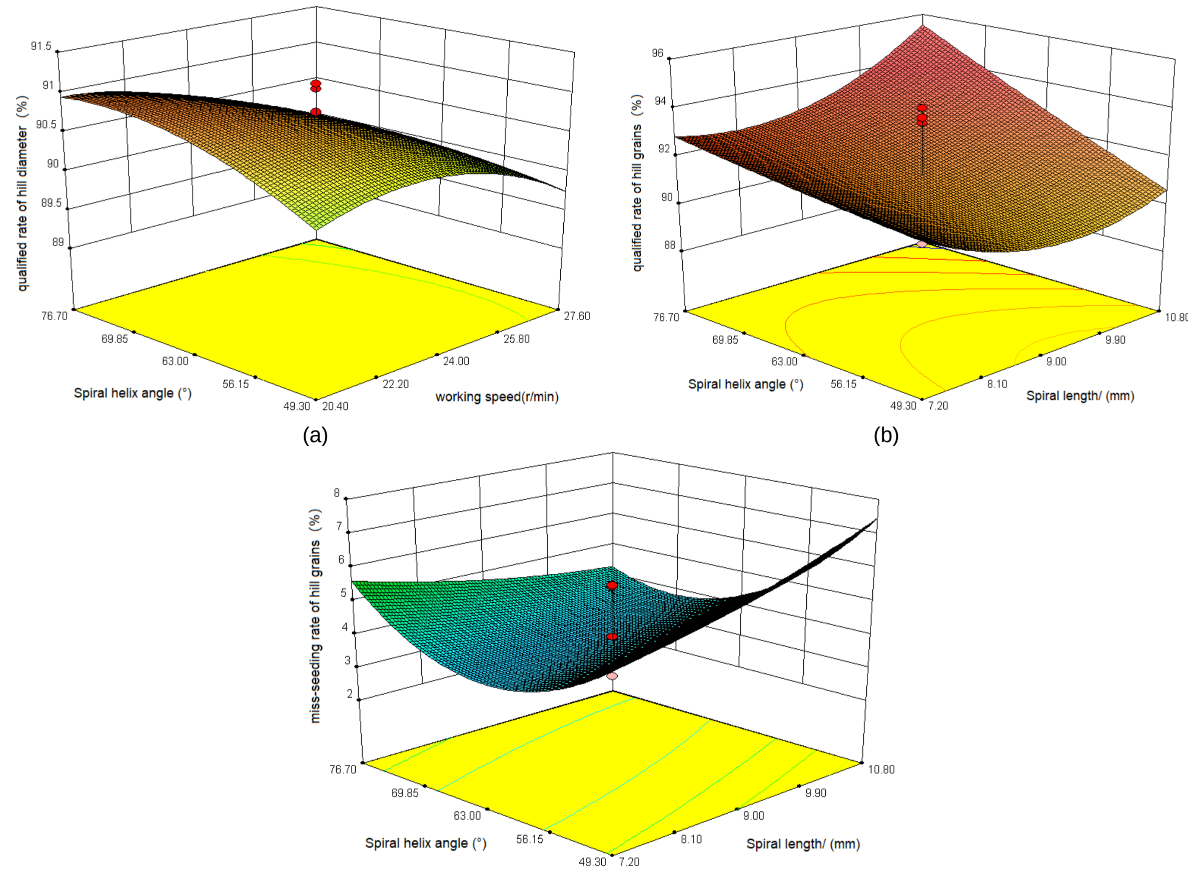


(a) (b) (c)

**Fig. 7 - Response surface graph**

### *Optimization and verification*

In order to obtain the optimal combination of test factors, a mathematical model is established based on the boundary conditions of the factors, and the regression equations on the qualified rate of hill diameters, the qualified rate of hill grains, and the miss-seeding rate of hill grains are analyzed. The mathematical model is as follows:

$$\begin{cases} \max \ y_1 \\ \max \ y_2 \\ \min \ y_3 \\ s.t. \quad 18 \le x_1 \le 30 \\ \quad\quad 6 \le x_2 \le 12 \\ \quad\quad 40 \le x_3 \le 86 \\ \quad\quad 0 \le y_1(x_1,\ x_2,\ x_3) \le 1 \\ \quad\quad 0 \le y_2(x_1,\ x_2,\ x_3) \le 1 \\ \quad\quad 0 \le y_3(x_1,\ x_2,\ x_3) \le 1 \end{cases} \tag{15}$$

When the working speed of the seed metering wheel is 23.2 r/min, the spiral groove length is 10.8mm and the helix angle of the spiral groove is 71.0°, the performance of the seed metering device is optimal. The qualified rate of hill diameter is 91.27%, the qualified rate of hill grains is 94.42% and the miss-seeding rate is 3.82% respectively.

According to the optimization results, the bench test is carried out, and the qualified rate of hill diameter is 91.06%, the qualified rate of hill grains is 94.64% and the miss-seeding rate is 3.64% respectively. The verification result is basically consistent with the optimization result, and the error is in an acceptable range.

## CONCLUSIONS

A seed metering device that can realize direct seeding of rice hill is designed. The key components of the seed metering wheel and spiral grooved spoon are studied, and Matlab software is used to analyze the movement state of rice buds in the spiral groove during the seeding process. The analysis shows that with the increase of the helix angle of spiral groove during the seeding process, the axial velocity of the rice buds first increases and then decreases, and the circumferential velocity gradually increases.

The quadratic regression-orthogonal rotation combination design is used to establish the mathematical model of experimental factors and seeding performance index. The response surface graph is analyzed to obtain the relationship of factors on the influencing trend and interaction of factors, and then the bench test is carried out. The results show that the optimization results and the verification results are basically the same.

Design-Expert 6.0.10 software is used to analyze the test results, and the regression model is optimized and verified. When the working speed of the metering wheel is 23.2r/min, the spiral groove length is 10.8mm, and the helix angle of spiral groove is 71.0°, the best combination is that the qualified rate of hill diameter is 91.06%, the qualified rate of hill grains is 94.64%, and the miss-seeding rate is 3.64%.

## ACKNOWLEDGEMENT

This work was supported by the National Natural Science Foundation of Zhejiang (No.LGN20E050005).

## REFERENCES

[1] Arzu Y., Adnan D. (2014). Measurement of seed spacing uniformity performance of a precision metering unit as function of the number of holes on vacuum plate. *Measurement*, vol.56, pp. 128-135.

[2] Cao C.M., Qin K., Wang A.M, et al. (2015). Design and Experimental Research on Rice Hill Seeder with Air-blowing Special Hole & Scoop-wheel Type. *Transactions of the Chinese Society for Agricultural Machinery*, vol.46, no.1, pp. 66-72.

[3] Dudarev I., Kirchuk R. (2017). Simulation of bulk materials separation process in spiral separator. *INMATEH - Agricultural Engineering*, vol.53, no.3, pp.57-64.

[4] He L.N., Zhao M.M., Zhao T.C., Hao X.Z., Zhang X.Z., He R.Y. (2019). Design and experiment of the spiral trough seed metering for rice and wheat. *Journal of Hunan Agricultural University (Natural Sciences)*, vol.45, no. 6, pp. 657-663.

[5] Hevko R.B., Baranovsky V.M., Lyashuk O.L., et al. (2008). The influence of bulk material flow on technical and economic performance of a screw conveyor. INMATEH - Agricultural Engineering, vol.56, no.3, pp. 175-184.

[6] Huang M., Fang S.L., Cao F.B., et al. (2020). Early sowing increases grain yield of machine-transplanted late-season rice under single-seed sowing. *Field Crops Research*, no.253, pp.107832. https://doi.org/10.1016/j.fcr.2020.107832

[7] Liu C.L., Li Y.N., Song J.N., et al. (2017). Simulation design and experiment of a directional seed-feeding device. *International Agricultural Engineering Journal*, vol.26, pp.16-24.

[8] Liu C.L., Wang Y.L., Du X., et al. (2019). Filling performance analysis and verification of cell-belt rice precision seed-metering based on friction and repeated filling principle. *Transactions of the CSAE*, vol.35, no.4, pp.29-36.

[9] Lu F.Y., Ma X., Qi L., Xing X.P., Li H.W., Guo L.J. (2018). Theory and Experiment on Vibrating Small-amount Rice Sowing Device. *Transactions of the Chinese Society for Agricultural Machinery*, vol.49, no.6, pp. 119-128,124.

[10] Luo X.W., Liu T., Jiang E.C., et al. (2007). Design and experiment of hill sowing wheel of precision rice direct-seeder. *Transactions of the Chines eSociety of Agricultural Engineering*, vol.23, no.3, pp.108-112.

[11] Ren W.T., Lü X.R., Kong A.J., et al. (2009). Development of the taped type rice direct seeding machine. *Journal of Shenyang Agricultural University*, vol.40, no. 1, pp.62-66.

[12] Trokhaniak O.M., Hevko R.B., Lyashuk O.L. et al. (2020). Research of the of bulk material movement process in the inactive zone between screw sections. *INMATEH - Agricultural Engineering*, vol. 60, no.1, pp.261-268.

[13] Vasylkovska K.V., Vasylkovskyi O.M., Sc. Sviren M.O. et al. (2019). Determining the parameters of the device for inertial removal of excess seed. *INMATEH - Agricultural Engineering*, vol. 57, no.1, pp.135-140.

[14] Wang Y.L., Zhu D.F., Xing J, et al. (2020). Characteristics of seedling raising and mechanized transplanting of hybrid rice with a low seeding rate by precise seeding method. *Chinese Journal of rice Science*, vol.34, no.4, pp. 332-338. DOI: 10.16819/j.1001-7216.2020.9113

[15] Xing H., Wang Z.M., Luo X.W., et al. (2020). Design and experimental analysis of the stirring device for pneumatic precision rice seed metering device. *Transactions of the ASABE*, vol.64, no.4, pp. 799-808. Doi: 10.13031/trans.13096

[16] Xing H., Ying Z., Wang Z.M, et al. (2018). Design of an active seed throwing and cleaning unit for pneumatic rice seed metering device. *International Journal of Agricultural and Biological Engineering*, vol.11, no.2, pp. 62-69. DOI: 10.25165/j.ijabe.20181102.3844

[17] Yang Y. (2020). Rice cultivation status and high yield cultivation suggestions. *Modern Agricultural Science and Technology*, vol.10, pp. 50-51.

[18] Yin Z.K. (2020). Experimental study on fixed distance and precision sowing of rice. *Hybrid rice*, vol.50, no. 1, pp.38-40.

[19] Zhang M.H., Wang Z.M, Luo X.W, et al. (2018). Review of precision rice hill-drop drilling technology and machine for paddy. *International Journal of Agricultural and Biological Engineering*, vol.1, no.3, pp.1-11. DOI: 10.25165/j.ijabe.20181103.4249

[20] Zhang S., Li Y., Wang H.Y., Liao J., Li Z.D, Zhu D.Q. (2020). Design and Experiment of U-shaped Cavity Type Precision Hill-drop Seed-metering Device for rice. *Transactions of the Chinese Society for Agricultural Machinery*, vol.51, no.10, pp. 98-108.

[21] Zheng J.X., Gao Y.Y., Yuan H.F., et al. (2018). Design of shaped-hole Volume-variable Precision seeder. *INMATEH - Agricultural Engineering,* vol. 56, no.3, pp.129-136.

[22] Zhou H.B., Liang Q.Y., Wen T.L., et al. (2016). Design and test of the quantitative seed feeding device with external groove wheel of two-stage vibration precision seed metering device. *Transactions of the Chinese Society for Agricultural Machinery*, vol.47, no. Supp, pp. 57-61.